# Radar Scatterometer Discrimination of Sea-Ice Types

S. K. PARASHAR, MEMBER, IEEE, ROBERT M. HARALICK, SENIOR MEMBER, IEEE, R. K. MOORE, FELLOW, IEEE, AND A. W. BIGGS, MEMBER, IEEE

Abstract-Experiments with 400-MHz and 13.3-GHz radar scatterometers indicate that these all-weather remote sensors provide some information which may be used to discriminate between some types of sea-ice categories. Using 12 incidence angles, first-year and multiyear ice were distinguished with greater than 90-percent correct identification accuracy on the basis of 13.3-GHz VV polarization scatterometer data taken in May 1967, near Pt. Barrow, Alaska (NASA Mission 47). Thin, first-year, and multiyear ice were distinguished with about 87-percent correct identification accuracy on the basis of the 13.3-GHz VV polarization scatterometer data taken in April 1970, also near Pt. Barrow, Alaska (NASA Mission 126) and about 75-percent correct identification accuracy on the basis of the 400-MHz VV polarization scatterometer taken during the same mission.

#### I. Introduction

THE DEVELOPMENT of remote-sensing radar systems operating in the microwave region of the spectrum has broadened the prospect of remote measurements of the significant features of the earth's surface. Radar systems are not sensitive to local weather conditions and they are not affected by the lack of incident light [1]. The all-weather day-night operational capability is particularly useful in regions such as the Arctic and Antarctic where light and weather conditions are uncertain most of the time.

About ten percent of the world's ocean is covered all or part of the year by ice. Weather conditions throughout the world are significantly influenced by variations of the sea-ice cover. Sea ice affects navigation in the Arctic and is, therefore, important both for shipping and for naval operations. A new interest is developing in the Arctic Ocean with the hope that it can be utilized more for navigational purposes, particularly as oil sources are located in the polar regions. A need exists to find the location and extent of open water and thin, thick, and very thick ice. Since sea ice covers such a large area, the only possible practical method is to sense the thickness of sea ice by remote techniques. This study was conducted to explore the possibility of utilizing radar systems for remote sensing of sea ice.

The results presented here, by analyzing radar scatterometer data taken in May 1967 (NASA Mission 47) and April 1970 (NASA Mission 126) near Pt. Barrow, Alaska, show that differentiation of sea-ice types by use of multiple radar backscatter measurements is feasible.

Most of the monitoring of sea-ice conditions in the future will undoubtedly be done with imaging sensors, particularly radars, because of the need to map large areas quickly. The

Manuscript received July 9, 1976; revised December 17, 1976.

S. K. Parashar was with the Remote Sensing Laboratory, University of Kansas, Lawrence, KS, He is now with the Canada Centre for Remote Sensing, Ottawa, Canada.

R. M. Haralick, R. K. Moore, and A. W. Biggs are with the Remote Sensing Laboratory, University of Kansas, Lawrence, KS.

main purpose of this study was to obtain information regarding the utility of and design parameters for such imaging radars. The imaging radar, however, provides information about each point on the surface at only a single angle of incidence. Thus the multiangle radar scatterometer obtains more information about each point and has the potential for superior identification of ice types; this information is, however, confined to a line beneath the radar. Use of an imaging radar and scatterometer together could give area coverage in which a strip with ice information better than that given by the imager alone would be provided. This additional information could allow a more accurate interpretation of the ice covered by the full radar image.

## II. RADAR SCATTEROMETER

When electromagnetic energy or waves hit the earth's surface, the waves may be transmitted, absorbed, specularly reflected, or scattered. The distribution of energy among these depends on the electrical properties of the target, the surface roughness and volumetric inhomogeneity of the target, the wavelength, and the angle of the incident electromagnetic wave. Signals returned along the same path as the incident energy are called backscatter. Such signals are the only component observed by the usual radar.

A radar scatterometer measures the backscattered signal [1] and permits determination of the radar scattering coefficient  $\sigma^{\circ}$  (radar cross section normalized to the illuminated area). The two radar scatterometers used in the NASA Earth Resources Aircraft Program experiments reported here operated at 13.3 GHz and 400 MHz. The NASA Mission 47 data were taken in May 1967 and the NASA Mission 126 data were taken in April 1970, near Pt. Barrow, Alaska. Both scatterometers use fan-beam antenna patterns in both the transmit and receive mode (Fig. 1). The 13.3-GHz scatterometer transmits a vertically polarized continuous-wave (CW) signal and collects a return signal from an illuminated region, which corresponds to ±60° along the flight line (along-track) and is 3° wide (across-track). The antenna beam for the 400-MHz scatterometer is also ±60° in the along-track direction and averages 7.5° in the across-track direction. The transmitted signals have both horizontal and vertical polar-Both like and cross-polarized measurements are made for each transmitted polarization. Because of the aircraft motion in the along-track plane, the radar returns at the different incidence angles are coded by Doppler-shift frequencies in the received signal frequency spectrum. The across-track dimension of a resolution cell is determined by the half-power points of the narrow beamwidth of the antenna. The along-track dimension of a resolution cell is determined by the bandwidth of a filter centered about the

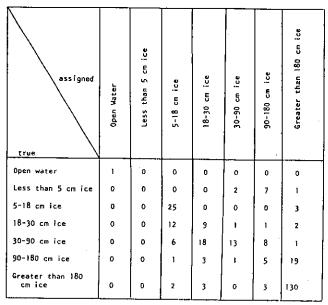


Fig. 1. Illustrates a contingency table for the prediction set using twelve angles of scatterometer data corresponding to 13.3 GHz and VV polarization. Rows are photographic categories and columns are radar categories assigned by a linear discriminant function decision rule (Mission 126). For category description see text.

Doppler frequency corresponding to a selected angle of incidence.

The radar differential scattering coefficient  $\sigma^{\circ}$  is calculated by solving the classical radar equation [1] for area targets, assuming that the variation across a resolution cell is negligible. The scattering cross-section signature (profile) for the surface is constructed by plotting  $\sigma^{\circ}$  as a function of incident angle  $\theta$ . Since  $\sigma^{\circ}$  for one area is measured at different times for different angles, the time must be scaled to yield a  $\sigma^{\circ}$  versus  $\theta$  plot for a particular path on the surface [1]. It is necessary to average returns from a modest range of angles to decrease the influence of fading. Hence, fine spatial resolution is incompatible with precise measurement of the amplitude. Plots of  $\sigma^{\circ}$  versus  $\theta$  and of  $\sigma^{\circ}$  versus time at a given  $\theta$  are both useful in analyzing an experimental data set.

For both 400-MHz and 13.3-GHz scatterometers, the dimension of the resolution cell in the along-track direction varies as a function of the incident angle. For an average aircraft ground speed of 100 m/s, the along-track resolution of the 13.3-GHz scatterometer necessary for precise measurement varies from about 33 m at 5° from vertical to 140 m at 60°. For the same aircraft ground speed and altitude, the along-track resolution for the 400-MHz scatterometer varies from 33 m at nadir (0°) to 285 m at 60°.

## III. SEA-ICE MORPHOLOGY

The formation of sea ice is a complex process that depends on a number of factors [2]: the brine content of the surface water (surface salinity, density of brine in the water), the vertical distribution of salinity, the surface temperature, the depth of the water, the wind, the currents, the wave conditions, and the rate of cooling.

Sea ice differs from fresh-water ice in that it has impurities in its matrix in the form of liquid brine inclusions. The salinity of sea ice is always less than the salinity of the original sea water because part of the brine trapped between ice crystals escapes during freezing.

In the spring and summer, sea ice starts melting. Continued thawing produces passages and holes in which surface water drains. First-year ice (less than one-year old) melts more readily than old ice, and is more salty than multiyear ice. Sea ice seldom becomes more than 2 m thick during the first winter. After the first year, this ice usually grows more than 2 m thick. Sea ice may attain much greater thicknesses in ridges and hummocks [3].

Both salinity and temperature profiles vary with the depth of the ice. These physical properties of sea ice, which change significantly with time and age, in turn determine its electrical properties. The complex permittivity depends on the amount of entrapped brine impurities present. The amount of trapped brine volume is related to salinity and temperature, both of which vary with depth. This implies that the complex permittivity also has a vertical profile. In addition, variation exists in the complex permittivity in the horizontal direction.

### IV. RADAR BACKSCATTER FROM SEA ICE

Radar backscatter from floating sea ice is a combination of scattering from ice-air and ice-sea-water interfaces and from irregularities within the ice mass. The relative contribution to backscatter from the boundaries and irregularities depends on the frequency and angle of the incident wave and the physical and electrical properties of sea ice such as surface roughness, temperature and salinity profiles, and thickness.

A theoretical study to determine the radar backscatter cross section  $\sigma^{\circ}$  for different types of sea ice at a 0.4- and 13.3-GHz frequency took the surface roughness into account and considered a vertical profile for complex permittivity with a small random horizontal variation [4]. The theoretical results were in general agreement with the experimental results obtained from Mission 126, which show that multiyear ice (greater than 180 cm thick) gives the strongest return at 13.3 GHz. First-year thin ice (18-90 cm thick) gives a much smaller return at 13.3 GHz. Very thin ice (less than 18 cm thick) gives the least return at 400 MHz. Water can be differentiated at both frequencies.

## V. SEA-ICE CLASSIFICATION

It was shown by Anderson [3] that the ages and relative thicknesses of sea-ice masses can be determined from stereoscopic aerial photography by using the tested and proven techniques of terrain air-photo analysis. Pattern configuration, tone, and surface features are used in interpreting sea-ice photographs.

Because of the variability in classification of ice types from aerial imagery by photo interpreters, surface information obtained by this method is subject to some unknown but significant error. This should be taken into account when interpreting any automatic classification where the ground truth was derived from manual interpretation of aerial photography.

Sea ice can be classified according to age, thickness, concentration, and formation. Sea ice for Missions 126 and 47 was classified according to age and thickness on the basis of surface roughness, shape, size, and texture. Sea ice for Mission 126 was classified initially into the following categories:

- 1) open water;
- 2) new ice or ice under 5 cm thick;
- 3) thin young ice (5-18 cm thick);
- 4) thick young ice (18-30 cm thick);
- 5) thin first-year ice (30-90 cm thick);
- 6) thick first-year ice (90-180 cm thick);
- 7) multiyear ice (greater than 180 cm thick).

Experiments with these seven categories did not show as effective discrimination as desired (Fig. 1). Thus we combined categories 2 and 3, 4 and 5, and 6 and 7.

Initially, sea ice for Mission 47 was divided into the following three major categories: water or thin ice, first-year ice, and multiyear ice. The surface area for each radarbackscattered return profile ( $\sigma^{\circ}$  versus  $\theta$ ) was assigned one of the above categories. Only profiles corresponding to homogeneous patches of sea ice were considered in the results presented here.

Each radar-backscattered return profile for Mission 47 contained values of  $(\sigma^{\circ})$  versus incidence angle  $\theta$ ) at incidence angles of 2.5, 5, 7, 15, 25, 35, 50, and 65° for 13.3-GHz VV polarization. Thus each backscattered profile consisted of an *n*-dimensional vector (measurement vector or profile), where *n* corresponds to the number of angles, nine in this case. These data were initially analyzed by Rouse [5], who assigned categories on the basis of single, rather than stereo, photographs. Rouse's categories were used as surface descriptors in this analysis.

Three hundred and sixty-three backscatter profiles were available for analysis. From these, 195 profiles were selected at random for the training set; the prediction (test) set consisted of the remaining 168 measurement profiles. For the training set, 25 profiles belonged to water or thin ice, 87 were from patches of first-year ice, and 83 were from patches of multiyear ice. The prediction (test) set consisted of nine profiles from water or thin ice, 81 from first-year ice, and 78 from multiyear ice.

To assign profiles to categories a simple Bayes rule was used. It assigns a measurement x to that category c having the highest conditional probability given x. Such a rule was constructed from the information available in the training set. The conditional probability of the measurement vector, given the category, was assumed to be of the multivariate normal form. Each measurement in the prediction set was assigned an ice category by the constructed decision rule. As a result, 92 percent of the measurements in the test set could be identified correctly [6]. The results are presented in Fig. 2(a).

In another experiment, the decision rule was formed differently. For each angle of incidence, the range of backscattered return was divided into three equal parts: small, medium, and large returns. Then, each component in the profile could take on only one of the three values: 0, 1, or

assigned true	Water, thin Ice	First-year ice	Multi-year ice
Water, thin ice	5	3	1
lst-year ice	4	71	6
Multi-year ice	. О	0	78

0-18cm thick	18-90cm thick	greater than 90cm thick
30	2	7
5	62	3
5	13	150
		30 2

(b)

assigned	0-18cm thick	18-90cm thick	greater than 90cm thick
0-18cm thick	32	6	1
18-90cm thick	5	55	10
greater than 90cm thick	1	10	157
	<u> </u>	(c)	

assigned

true

0-18cm thick 18-90cm thick greater than 90cm thick

0-18cm thick 30 12 7

18-90cm thick 16 51 38

greater than 90cm thick 1 23 207

Fig. 2. Radar scatterometer (VV polarization) classification of ice types. (Rows are photographic categories and columns are radar categories.) (a) Radar frequency=13.3 GHz; Bayes decision rule, nine angles of incidence. (b) Radar frequency=13.3 GHz; linear decision rule, 12 angles of incidence. (c) Radar frequency=13.3 GHz; nearest neighbor rule, 12 angles of incidence. (d) Radar frequency=400 MHz; linear decision rule, 12 angles of incidence.

2. Using every other profile for the training set, a simple nearest neighbor rule was constructed. The nearest neighbor rule assigns a measurement in the test set to that category of measurement in the training set which is closest to it in n space [7]. Eighty-one percent of the measurements in the test set could be correctly classified with this decision rule.

By using only the values of  $\sigma^{\circ}$  from those incidence angles greater than 15°, about 79 percent of the measurements were correctly classified for experiment one; about 75 percent, for experiment two. By dividing the first-year ice into three subtypes, a correct classification of 75 percent was achieved.

The radar scatterometer data collected during Mission 126 corresponded to a 13.3-GHz VV polarization and a 400-MHz, multipolarization (VV, HH, HV, and VH). The scatterometer data or the value of radar backscatter coefficient  $\sigma^{\circ}$  were available for 12 forward angles: 5, 10, 15, 20, 25, 30, 35, 40, 45, 50, 55, and 60° for 13.3 GHz; and 0, 5, 15, 20, 25, 30, 35, 40, 45, 50, and 60° for 400 MHz. The surface classifications for these observations were based on stereophoto analysis by Parashar, working initially with and under the tutelage of Anderson.

For Mission 126 data analysis, a linear decision rule was used to separate each pair of categories. The pairwise linear

decision rule assigns category one to a measurement x if w'x > 0. Otherwise, it assigns category two to x. The weight vector w of the discriminant function w'x can be constructed from the training data using a regression method as follows. Let D be the training data matrix. Its first N rows are the training vectors from category one. Its last M rows are the training vectors from category two. Let T be a column vector whose first N components are +1 and whose last M components are -1. Then the least square method of solving T = Dw gives  $w = (D'D)^{-1}DT$ , the normal equation for its solution.

With seven categories there are 21 linear discriminant functions. The data profiles in the test set were classified on the basis of a majority vote of these discriminant functions. From the 558 backscatter profile measurements at 13.3 GHz, 281 were selected for the training set and the remaining 277 belonged to the prediction set. About 66 percent of the measurements were correctly identified into the seven categories of ice [4]. By using six alternate angles instead of 12, a correct classification of 64 percent was achieved.

A less demanding discrimination was then attempted between thin first-year ice (less than 18 cm thick), thick firstyear ice (between 18 and 90 cm thick), and thick first-year or multiyear ice (greater than 90 cm thick). From the data sample of 556 measurements, 270 were selected for the training set and the remaining 277, for the test set. Each measurement in the prediction set was assigned an ice category by a majority vote of the linear decision rule. Fig. 2(b) illustrates the resulting contingency table of "true" ice identification (photographic) versus assigned ice identification. About 87 percent of the assignments were correctly classified. By using only six alternate angles instead of 12, a correct classification of 86 percent would be achieved [4]. Using the same training and testing sets, a nearest neighbor rule gave 88-percent correct classification when all 12 angles were used (Fig. 2(c)).

In another experiment the F method for nonparametric tests was used to estimate the percentage of correct classification for the reduced category data. This method is given in detail by Lissac and Fu [9]. It consists of finding the optimum separability measure between the categories. To implement such a method an estimate is required of the conditional probability density of the measurement, given the category for a nonparametric case. The density estimation scheme as given by Loftsgaarden and Quesenberry [10] was utilized to find such expressions. The probability of correct classification is given by (Lissac and Fu [9]):

$$\hat{P}_{c} = \frac{1}{N} \sum_{j=1}^{N} \frac{\|X_{j} - X_{jmk}\|^{-L}}{\sum_{j=1}^{M} \left\{ \|X_{j} - X_{jik}\| \right\}^{-L}}$$

where N

Ntotal number of samples; L dimensions of each sample;  $X_1, \dots, X_N$  L-dimensional samples; M number of categories or classes;  $X_{ijk}$  kth sample closest to  $X_j$  from all samples in category i;

and m is an index such that

$$||X_i - X_{imk}|| < ||X_i - X_{iik}||$$
, for all i.

The above method can be implemented by finding the L-dimensional distance from sample j to all the other samples. Then for each class or category find the kth closest sample, where  $k = (n_i)^{1/2}$  and  $n_i$  is the total number of measurements in the class i. The sum of these distances for all the categories  $i = 1, \dots, M$  will give the denominator. The minimum of these distances will be the numerator. Repeat the above for all samples  $j = 1, \dots, N$  and add the resultant numbers to find the probability of correct classification. By implementing such a method a correct classification of 96.5 percent was estimated.

The data at 400 MHz corresponded to four polarizations (VV, HH, VH, and HV). From a data sample of 700, 385 measurements were selected for the training set. Of these, 229 belonged to thick first-year or multiyear ice (greater than 90 cm thick), 105 were first-year ice (18-90 cm thick), and 51 were from thin first-year ice (less than 18 cm thick). The prediction set consisted of the remaining 385 measurements. A linear decision rule was constructed on the basis of information available in the training set. Each measurement in the prediction set was assigned an ice category. The resulting contingency table of true ice identification versus assigned ice identification for VV polarization is given in Fig. 2(d) when all 12 angles were considered. About 75 percent of the measurements were classified correctly when 12 angles were considered and about 62 percent, when only six angles were used.

## VI. CONCLUSION

A multiangle 13.3-GHz vertically polarized radar scatterometer is able to distinguish sea ice types better than the 400-MHz scatterometer. Using a Bayes decision rule assuming a multivariate density function, the 13.3-GHz scatterometer achieved a 92-percent correct identification accuracy in distinguishing water or thin ice, first-year ice, and multiyear ice. Other automatic classifying techniques had identification accuracies just less than 90 percent for the 13.3-GHz scatterometer.

## REFERENCES

- R. K. Moore, "Microwave remote sensors," in Manual of Remote Sensing, vol. 1, Robert Reeves, Ed., American Society of Photogrammetry, Falls Church, VA, ch. 9, pp. 399-537.
- [2] P. Groen, The Waters of the Sea. London: D. Van Nostrand Co. Ltd., 1967.
- [3] V. H. Anderson, "Sea ice pressure ridge study: An airphoto analysis," in *Photogrammetria*. Amsterdam: Elsevier Publishing Company, 1970.
- [4] S. K. Parashar, "Investigation of radar discrimination of sea ice," (Ph.D. dissertation), The University of Kansas Center for Research, Inc., Remote Sensing Laboratory, Lawrence, KS, Tech. Rep. 185-13, May 1974.
- [5] J. W. Rouse, "Arctic ice type identification by radar," Proc. IEEE, vol. 57, pp. 605-611, Apr. 1969.
- [6] A. W. Biggs, R. M. Haralick, and R. K. Moore, "Sea ice discrimination with radar scatterometers," The University of Kansas Center for Research, Inc., Remote Sensing Laboratory, Lawrence, KS, Tech. Memo. 185-1, Jan. 1971.

- [7] R. O. Duda and P. E. Hart, Pattern Classification and Scene Analysis. New York: Wiley, 1973.
- [8] K. Fukunaga, Introduction to Statistical Pattern Recognition. New York: Academic Press, 1972.
- [9] T. Lissack and K. S. Fu, Error Estimation and its Applications
- to Feature Extraction in Pattern Recognition, TR-EE73-25, Purdue University, 1973.
- [10] D. O. Loftsgaarden and C. P. Quesenberry, "A nonparametric estimate of a multivariate density function," Ann. Math. Statistics, vol. 36, pp. 1049-1051, 1975.